3D Printed Galilean Telescope for Low-Vision Patients †

Daniel Aguirre-Aguirre [1,2,*], Itzel Muñoz-Juárez [3], Martin Isaías Rodríguez-Rodríguez [3], Brenda Villalobos-Mendoza [4], Ruth Eva Hernández-Carbajal [3], Rufino Díaz-Uribe [1] and Rafael Izazaga-Pérez [5]

1 Instituto de Ciencias Aplicadas y Tecnología, Universidad Nacional Autónoma de México, Cd. Universitaria, Apdo. Postal 70-186, Mexico City 04510, Mexico; rufino.diaz@icat.unam.mx
2 Unidad de Investigación y Tecnología Aplicadas, Universidad Nacional Autónoma de México, Vía de la Innovación No. 410, Autopista Monterrey-Aeropuerto Km. 10, PIIT, Cd. Apodaca 66629, Mexico
3 Carrera de Optometría Facultad de Estudios Superiores Iztacala, Universidad Nacional Autónoma de México, Avenida de los Barrios No. 1 los Reyes Iztacala, Tlanepantla 54090, Mexico; itzel.mzjz3@gmail.com (I.M.-J.); martin.isaias.rodriguez@iztacala.unam.mx (M.I.R.-R.); ruth.hernandez.carbajal@iztacala.unam.mx (R.E.H.-C.)
4 Departamento de Física y Matemáticas, Universidad de Monterrey, Av. Ignacio Morones Prieto 4500 Pte., San Pedro Garza García 66238, Mexico; brenda.villalobos@udem.edu
5 Dirección de Investigación y Desarrollo Tecnológico, Centro de Integración Tecnológica, Instituto Nacional de Astrofísica, Óptica y Electrónica, Luis Enrique Erro #1, Sta. María Tonantzintla, San Andrés Cholula 72840, Mexico; izazagax@inaoep.mx
* Correspondence: daniel.aguirre@icat.unam.mx
† This article is an extended version of the paper originally published in the proceedings of ACONTACS 2023: "Desempeño de telescopios galileanos en pacientes informados con diagnóstico de baja visión," ACONTACS 2023, 5, 62–72.

Abstract

Low vision is a condition in which a person experiences a significant loss of visual acuity or visual field that ordinary glasses, surgery, or medication cannot correct. Individuals suffering from this condition struggle to perform daily tasks, even when using glasses or contact lenses. In some cases, telescopes are recommended for patients with low vision diagnosis because they could help them improve their quality of life. Therefore, we propose a 3D-printed Galilean telescope for low-vision patients, accessible to both the vulnerable and nonvulnerable sectors of the population, with the advantages that the fabrication time, cost, and weight are considerably reduced. The performance of the 3D-printed Galilean telescope was evaluated by comparing it to an identical N-BK7 glass Galilean telescope design, obtaining a difference of 0.49 lp/mm in optical resolution. Clinical results from a patient with low vision, obtained as part of a proof-of-concept study, showed that the 3D-printed Galilean telescope improved the patient's visual acuity, increasing it by up to 4 lines on the LEA numbers, from 10/80 to 10/32. Additionally, the 3D telescope enhanced the patient's contrast sensitivity, improving it from 6 cpd (cycles per degree) level 8 to 18 cpd level 4.

Keywords: 3D printing; low vision; Galilean telescope

1. Introduction

According to the World Health Organization (WHO), at least 2200 million people have one vision impairment (VI), among whom 1000 million cases could have been prevented. Besides this, most eye conditions are higher in low- and middle-income countries, and further so in underserved populations [1–3]. As reported by the WHO and the International Classification of Diseases ICD-11 [4], visual impairment occurs when an eye condition, such as age-related macular degeneration, cataract, corneal opacity, diabetic retinopathy,

glaucoma, refractive error, or trachoma, affects the visual system and one or more of its vision functions, such as as visual acuity (VA), color vision, stereopsis/binocular vision (depth perception), contrast sensitivity, and/or vision in the peripheral visual fields [5–8]. The diagnosis of VI is realized through a non-invasive and simple measurement of VA. The test consists of discerning two high-contrast points in space by using an optometric chart placed at a fixed position (6 m or 20 feet) [1,9,10].

Commonly, visual impairment is classified into two different groups, measuring the visual acuity in the better eye. The first group is distance VI, which could have the levels of: (a) mild, VA > 20/40 and ≤20/70; (b) moderate, VA > 20/70 and ≤20/200; (c) severe, VA > 20/200 and ≤20/400; (d) blindness, >20/400 and ≤20/1200 or counts fingers (CF) at 1 m; (e) blindness, >20/1200 and light perception; and (f) blindness, no light perception. The second group is near VI, with VA > N6 or M 0.8 at 40 cm [4,11]. Following the data reported by the Pan American Health Organization (PAHO), in the first group, 217 million people have distance VI from moderate to severe, which, based on the European Council of Optometry and Optics (ECOO), is defined or diagnosed as low vision (LV) [1,11]. Low vision cannot be corrected by ordinary glasses, surgery, or medication, which limits daily activities such as reading, writing, recognition of faces and facial expressions, and safe walking and movement, among many others [12–14]. However, LV patients can improve their quality of life by using optical devices like telescopes and specific visual aids, which boost their functionality and enable them to maintain a certain degree of independence.

On the other hand, the versatility of 3D printing to fabricate custom pieces with high precision, low cost, and reduced time allows adapting this technology to the needs of each user. Hence, it is not surprising that 3D printing has experienced rapid growth in scientific, technological, and medical fields. For instance, in medical applications, orthopedic and cranial implants [15], surgical instruments [16], and external prostheses [17] are some areas where additive tech has been implemented. The low manufacturing costs compared to traditional fabrication methods and the ability to generate accurate anatomical models for surgical planning and medical training are some of its advantages. Also, 3D printing enables the use of a wide variety of biomedical materials [18,19], including biocompatible polymers [20], ceramics, and metals [15], ensuring compatibility with the human body and reducing rejection risks. In ophthalmology, 3D printing has also had a significant impact, where it has facilitated the creation of indirect ophthalmoscopes [21], intraocular lenses [22], and specialized optical devices [23], allowing the exploration of new materials and optical geometries that optimize the efficiency of visual aids and offering innovative solutions to improve the quality of life of people with visual impairment. These, and the earlier mentioned advantages of precise and rapid manufacturing of lenses and optical devices, are just some of many reasons why 3D printing has emerged as a promising tool in optics applied to visual rehabilitation. Therefore, we propose a 3D-printed Galilean telescope (GT) for low-vision patients, accessible to both the vulnerable and nonvulnerable sectors of the population, which can contribute to the Sustainable Development Goals (SGD 3) for achieving universal health coverage, with the advantages that fabrication times, costs, and weight are considerably reduced. Also, we want to demonstrate that 3D-printed lenses can be used directly in medical instrumentation and not just as prototypes, besides contributing to new strategies in the design and accessible optical device manufacturing. In previous work [24–28], we showed that optical lenses, including spherical, aspherical, and freeform designs, can be easily and rapidly fabricated using additive technology. Hence, in this paper, we report the fabrication of a complete Galilean telescope—including both the lenses and the tube—using the commercial FormLabs Form 3 3D printer with high-resolution stereolithography (SLA) technology and Clear Resin V4.0 from the same company. Its optical performance was evaluated by comparing the 3D-printed GT to a N-BK7 glass GT

assembled from the LSB04 Thorlabs lens kit. To test its clinical functionality, the device was evaluated by a patient with low vision as part of a proof-of-concept study. The patient demonstrated a significant improvement in vision—from 10/80 to 10/32 in visual acuity and from 6 cpd level 8 to 18 cpd level 4 in contrast sensitivity. The work is organized as follows: a brief introduction about low vision and the importance of 3D printing in recent years is presented in Section 1; the optical and mechanical parameters used for the lenses and the telescope's tube fabrication are described in Section 2; the instrument's optical functionality is shown in Section 3; the instrument's clinical tests are shown in Section 4; and finally, in Section 5, the conclusions and final comments are presented.

2. Galilean Telescope Fabrication

The tube and lenses of the Galilean telescope were entirely 3D printed using the FormLabs Form 3 commercial 3D printer, which employs high-resolution stereolithography (SLA) technology and Clear Resin V4.0 from the same company [29–31]. To evaluate the optical quality and dimensional accuracy of the fabricated components, geometric parameters such as radii of curvature, diameters, and surface figure were carefully measured. Additionally, since the roughness of 3D-printed surfaces may influence light scattering and thus affect the final image quality, it was also assessed during the functionality tests, particularly on these printed elements. The following sections describe the optical and mechanical parameters used, as well as the fabrication process.

2.1. Lens Selection

A Galilean telescope with a power of magnification of 2× is the most common, simple, and recommended visual aid for low vision patients [32–34]. It is for this reason that, in this work, we followed its design for the fabrication of the telescope. Also, Galilean telescopes are compact and lightweight systems that are easy to assemble in glasses, allowing LV patients to improve their distance vision through practical and non-voluminous devices. Moreover, GT's low-power optics provide a large visual field, compared to bigger magnification telescopes, facilitating orientation and the patient's safe walking and movement. The power of magnification of 2× was obtained by using two N-BK7 glass lenses, taken from the LSB04 Thorlabs lens kit, the LA1509-A planoconvex lens, and the LC1715-A planoconcave lens. The optical parameters of the lenses are summarized in Table 1, and the corresponding optical design is shown in Figure 1a.

Table 1. Geometrical parameters of glass and resin lenses.

	Eyepiece Lens (mm)	Objective Lens (mm)
Thorlabs code	LC1715	LA1509
Diameter	25.4	25.4
Focal length	−50	100
Radius of curvature Surface #1	−25.7	51.5
Radius of curvature Surface #2	Inf.	Inf.
Central thickness	2	3

Figure 1 presents spot diagrams corresponding to different field angles for both the glass and resin Galilean telescopes. As expected, chromatic aberration was present in both designs due to the use of singlet lenses, with more noticeable dispersion observed in the resin telescope. This increase in chromatic aberration was attributed to the lower Abbe number and refractive index variations of the 3D-printed resin material. Despite the presence of chromatic aberration, its impact on the visual performance of low-vision

patients was negligible, as the color fringes remained below the threshold of perceptibility for the intended application. It is important to note that changes in the refractive index in the optical model led to variations in the focal length of both lenses, requiring adjustments to their separation to achieve an afocal system. Therefore, both telescope designs remain viable for clinical use.
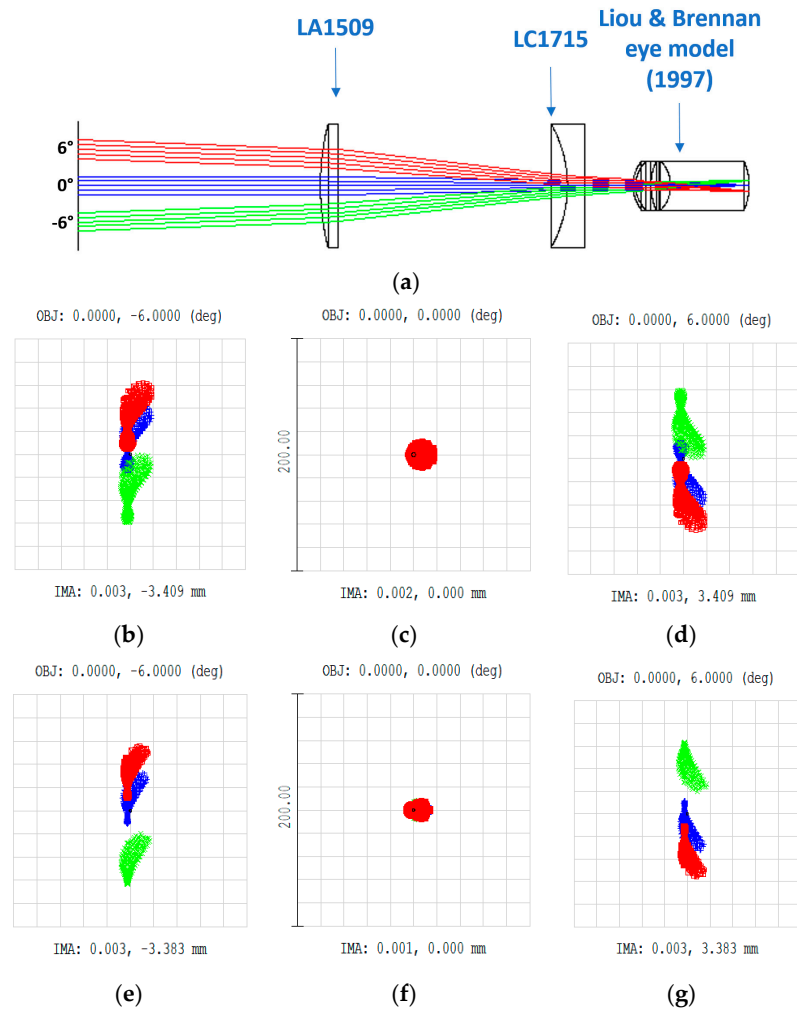
Figure 1. Galilean telescope: (**a**) Zemax ray tracing. Spot diagrams fields (**b**,**e**) 6 degrees, (**c**,**f**) 0 degrees, and (**d**,**g**) −6 degrees, for glass and resin telescopes, respectively. Wavelengths: 486.1 nm (blue), 587.6 nm (green), and 656.3 nm (red).

To ensure faithful reproduction of the required optical specifications in the 3D-printed lenses, the optical parameters of Table 1 were input into AutoCAD 2026 to obtain the lenses' rendering (Figure 2a). The CAD models were then sent to the 3D printer to initiate the printing process. This involved preparing the files in the printer's software, setting the appropriate parameters, such as a layer thickness of 25 microns and a print orientation angle of 30 degrees, and ensuring the printer was calibrated for optimal accuracy. Once these steps were completed, the 3D printer fabricated the components layer by layer according to the digital designs.

When the 3D printing of the lenses was finished, they were post-processed. First, they were exhaustively washed in Form Wash to remove all traces of unsolidified resin. Then, they passed a final curing process in Form Cure to maximize their strength and stability [26] (Figure 2b). Finally, the lenses were polished using the conventional method in specialized optical polishing machines (Figure 2c). The polishing process enhanced the optical surface

quality, significantly reduced light dispersion, and optimized lens transmittance. This process, performed at the INAOE's Optical Workshop, is described next.
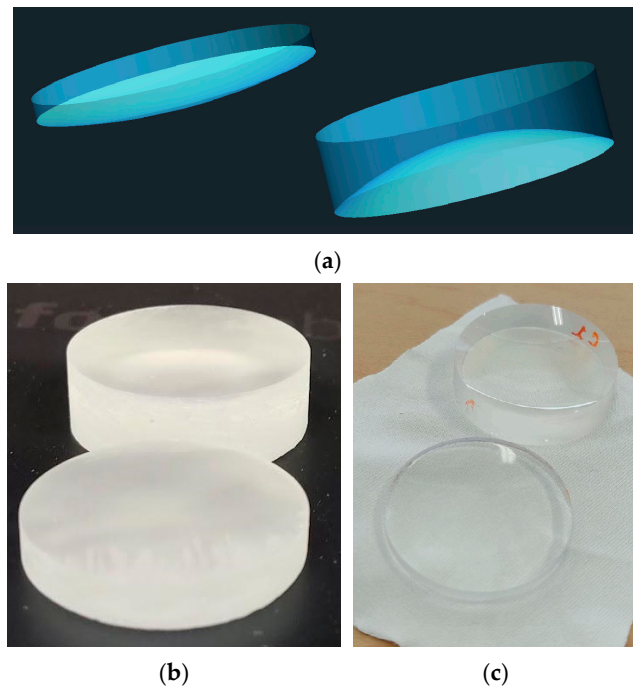
Figure 2. Design and fabrication. (**a**) CAD design, (**b**) lens curing, and (**c**) polished lens.

2.2. Optical Fabrication

The lenses were polished using a Strasbaugh® 6DA-DC4 polishing machine. To perform the grinding process, the lens was mounted on the machine's overarm with a glass tool positioned below it on the rotating axis (Figure 3a). The inverted configuration helped to maintain symmetric material removal, considering the resin's density (Table 2).
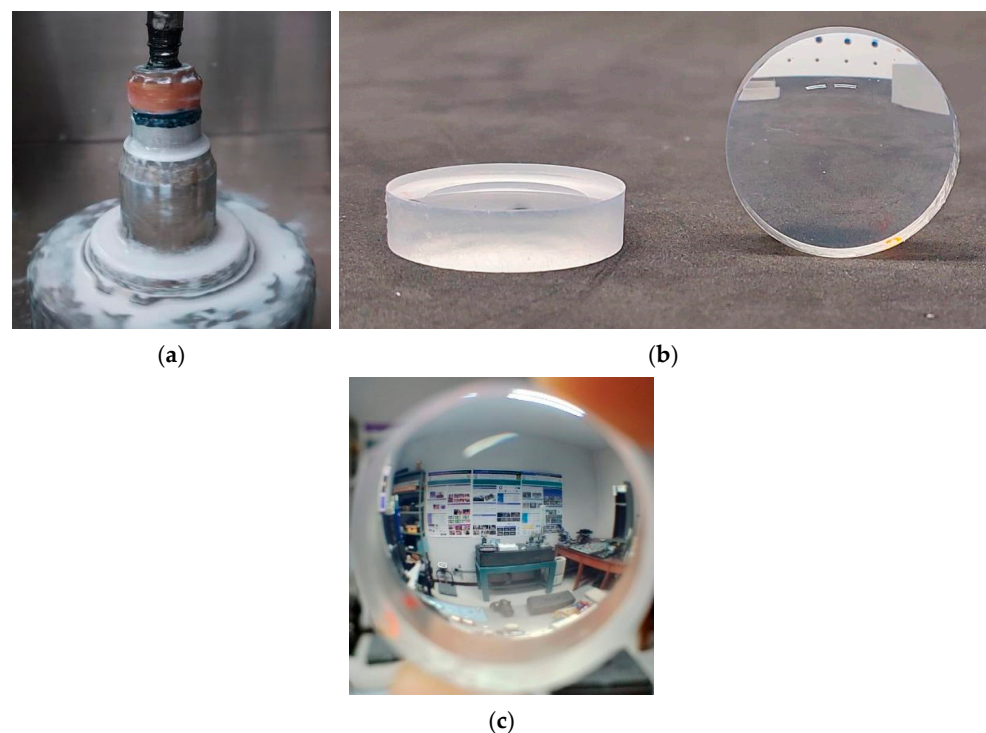
Figure 3. Polishing. (**a**) Rotating axis, and (**b**,**c**) lenses after polishing stage.

Table 2. Mechanical and optical resin properties.

Parameter	Value
Density (g/cm^3)	1.15
Thermal expansion (μm/m-°C)	122.4
Tensile modulus (GPa)	2.8
Friction coefficient	0.48
Solvent resistance (IPA weight gain) %	<1.0
Index of refraction (D line)	1.505

The resin parameters are critical for understanding the polishing process, ensuring low irregularity, and achieving high surface quality. A surface finish roughness of approximately 15 microns was achieved for the grinding stage. The next stage was the polishing process, which is critical due to the challenges of polishing soft materials such as resin. This stage was also performed in the Strasbaugh® 6DA-DC4 polishing machine; a polishing pad to balance between density and solvent resistance, ensuring compatibility with the resin, was used. The pad was a POLITEX™ polyurethane pad from Pureon; the polishing compound was Kontax 602 from Universal Photonics, a high-purity alumina formulation specifically designed for plastic materials. Figure 3b shows the results for the resin lenses after polishing.

When the polishing process was finished, a completely reflecting, transparent, and smooth surface was observed (Figure 3c). The irregularity measurements of the lens surfaces were performed using a Zygo Mark II interferometer. The 3D-printed lenses were tested using two reference surfaces: a flat surface for the two flat surfaces, and a sphere for the concave and convex surfaces; both reference surfaces had a precision of PV = $\lambda/20 \approx 32$ nm ($\lambda = 632.8$ nm). The measured irregularity for the spherical surfaces was 4.45λ peak-to-valley (PV) and 0.81λ root mean square (RMS) for the eyepiece and 4.53λ PV and 0.76λ RMS for the objective. For the flat surfaces, the measured irregularity was 6.83λ PV and 1.17λ RMS for the eyepiece and 8.23λ PV and 1.52λ RMS for the objective lens.

The radius of curvature was measured using the same interferometer in linear mode, along with a digital scale from Easson™, attached to a precision linear rail, which was used to displace the lens and to determine the distance between the vertex and the center of curvature position. The radii of curvature for the spherical surfaces were −25.83 mm and 51.9 mm for the eyepiece and objective lenses, respectively. Additionally, the diameters and thickness of the 3D-printed lenses were measured using a Mitutoyo digital caliper. The diameter and thickness were 25.42 mm and 2.05 mm for the eyepiece and 3.10 mm and 25.43 mm for the objective, respectively. Next, roughness measurements are described.

2.3. Roughness

A Linnik interferometer [35,36], with two Edmund Optics lenses of 25 mm fixed focal length and a numerical aperture of 0.0306, placed in both arms of the interferometer, was used to measure the surface roughness from the resin lenses (Figure 4).

Figure 5a shows one of the interferograms obtained with the Linnik interferometer for the roughness measurements, and Figure 5b shows one roughness profile of the surfaces under test. It is worth mentioning that this measurement was realized over a length l_m of 21.21 μm, corresponding to the size of the spot generated by the 25 mm fixed focal length lens used in the Linnik interferometer.
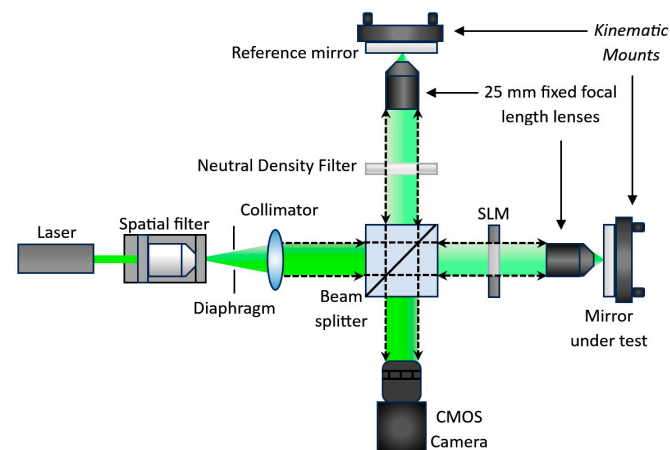
Figure 4. Roughness measurement in the Linnik interferometer.

(**a**)   (**b**)
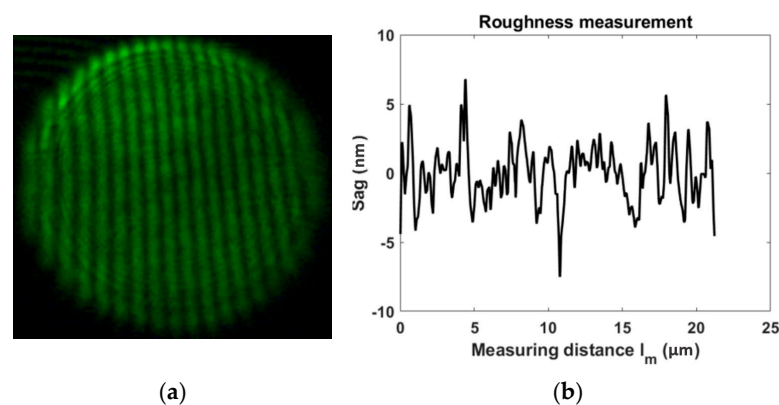
Figure 5. Roughness. (**a**) Interferogram, and (**b**) roughness profile.

The roughness average (Ra) for the 3D-printed lens with the surface finish polished using the traditional method was 1.569 nm ± 0.35 nm. The peak-to-valley (PV) measurement was 14.237 nm ± 3.41 nm. Note that these values aligned with the roughness characteristic of printed surfaces [37]. Next, the design and mechanical parameters of the telescopes' tubes are described.

2.4. Tube Design

For assembling the two Galilean telescopes (the 3D-printed and the N-BK7 glass), customized tubes were also designed in AutoCAD [38]. The tubes were created to provide adequate support for the lenses during the user's handling. The principal function of the tubes was to optimize and provide a better user experience for patients (Figure 6).

The ergonomics of the telescope was a special parameter considered during the design of the tubes. Thus, the tubes were designed with texturized surfaces to enhance adherence, which is a very useful characteristic for visually impaired people. The tube design's texture facilitates holding and handling of the telescope, reducing the risk of slipping and allowing more intuitive use (Figure 7). The tube had a 70.5 mm maximal length stretched and 53.5 mm minimal length compressed. The design incorporated a threaded adjustment mechanism that allows easy-to-use focusing with a 17 mm range (See Supplementary Materials for additional data). Furthermore, the adjustment had a linear travel of one millimeter per turn, providing precise and gradual control, so users could adapt the focus to their specific visual needs. This feature is practical and highly beneficial for patients with low vision because it allows them to optimize their visual experience without requiring sudden movements or complex adjustments.
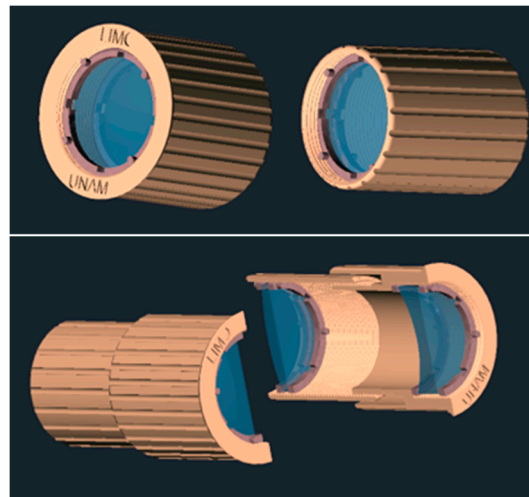
Figure 6. Telescope tube rendering.
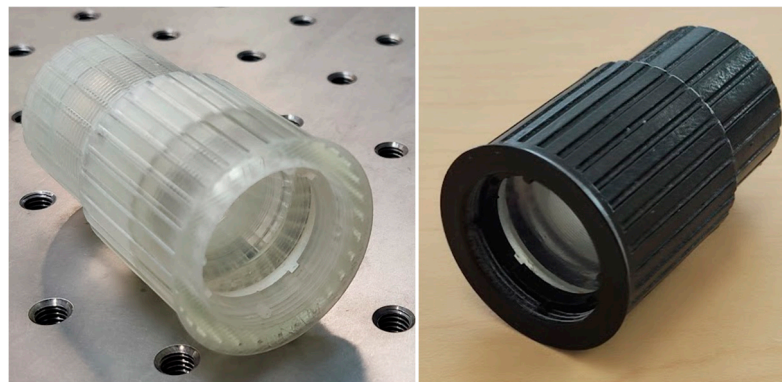
Figure 7. Low-vision Galilean telescope fabricated 100% with clear resin.

To eliminate spurious light that could affect the telescope's performance, a black paint coating was applied to it (Figure 7). The paint coating minimizes unwanted internal reflections, enhances contrast and image quality, and contributes to the care and material's durability, ensuring the telescope's appropriate performance within different use conditions. Following, the instrument functionality tests are presented.

3. Instrument Optical Functionality

To evaluate the 3D-printed GT's functionality, its optical performance was compared to that of a N-BK7 glass GT. As was earlier mentioned, the optical parameters of the 3D-printed GT were defined from the design obtained for the N-BK7 glass GT assembled from the LSB04 Thorlabs lens kit, with the LA1509-A planoconvex lens, and the LC1715-A planoconcave lens, see Table 1. The characterization of the instrument included optical resolution tests, angular magnification, and field of view. Next, the results for evaluating the viability of using 3D-printed lenses in visual aid applications for low-vision patients are shown.

3.1. Optical Resolution

The telescopes' optical resolution analysis was realized using the standard USAF 1951 resolution target and an Edmund Optics OE-18112 camera from IDS Imaging, Germany, with 18.1 megapixels. The distance between the camera and the target was adjusted to ensure that the target filled the entire field of view of the camera. The experimental

setup configuration allowed a precise optical performance evaluation by measuring the instruments' ability to resolve fine details in the resolution target.

We observed that, for the glass lenses telescope, the maximum resolution achieved was 4.49 lp/mm, as the bars of group 2, element 2, were perceptible (see Figure 8a). By comparison, the resin lenses telescope reached a maximum resolution of 4.00 lp/mm, with the bars of group 2, element 1, being discernible (see Figure 8b). Note that the differences in optical resolution between the analyzed telescopes were relatively small, which led to obtaining very similar images. The two instruments showed the capability to discern fine details, which is essential for low-vision patients. As can be seen, the two models had very similar optical performance, which indicated that, regardless of the lens used, the telescopes effectively enhanced object visibility and could assist patients to improve their quality of life. Note that the differences in the values obtained for the instruments' resolution were not significant enough to affect what the patient distinguishes, allowing the two telescopes to be considered viable options for adapting optical aids. Next, the optical parameters of the telescopes are presented, focusing on key aspects such as angular magnification and field of view, which determine the system's visual performance.
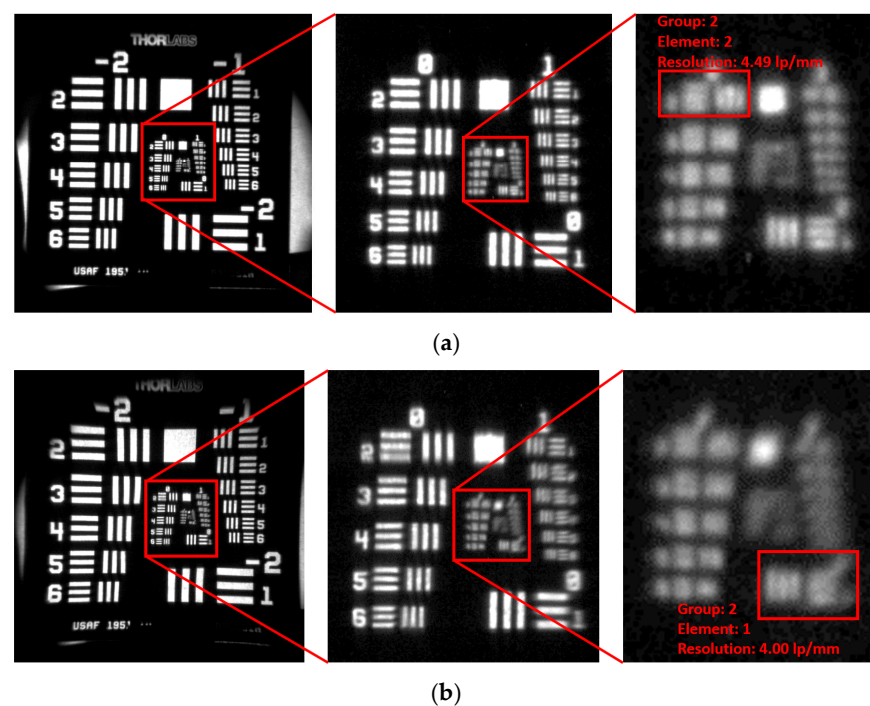
Figure 8. Telescope resolution analysis. (**a**) N-BK7 glass lenses, and (**b**) resin lenses.

3.2. Optical Parameters

The optical performance of the Galilean telescopes was evaluated in terms of angular magnification and field of view, two critical parameters in visual aid systems (see Table 3). The angular magnification was determined using Zemax (Ansys Zemax OpticStudio 2023), based on the focal lengths of the objective and eyepiece lenses calculated from the measured curvature radii (see Section 2.2). The nominal magnification for both telescopes is shown in Table 3. The field of view was estimated by measuring the angular extent of the scene visible through the telescope, as described in references [38,39], which is inherently limited in Galilean designs due to the negative eyepieces. Despite this limitation, the resulting field of view was sufficient for practical use in mobility and reading tasks, making the system suitable for patients with low vision.

Table 3. Optical parameters.

	Glass Telescope	Resin Telescope
Amplification	1.94×	1.96×
Field of view (FOV)	11.31°	10.31°

Following this, the clinical functionality of the instruments is described in detail, including an evaluation of their effectiveness in improving visual performance in patients with low vision. This section discusses the outcomes of clinical tests and measurable improvements in visual acuity and contrast sensitivity achieved with the use of telescopes.

4. Instruments' Clinical Functionality

The development of accessible optical devices for low-vision patients, especially those in vulnerable sectors, is a real need that must be attended. On this matter, this work seeks to contribute to new strategies in the design and manufacture of instruments that are useful for this sector of the population. In this section, we describe the tests conducted as part of a proof-of-concept study to evaluate and adapt the 3D-printed Galilean telescope for a 75-year-old female patient, who provided informed consent and was diagnosed with myopia magna, pseudophakia, ocular infarction with hemorrhage, retinal thinning, retinal detachment in the right eye, and central scotoma in the same eye. The instruments used in this study were specifically adapted to enhance the patient's visual acuity and contrast sensitivity, two key factors that must be corrected to improve vision functions for individuals with visual impairments. The complete patient data are shown in Table 4.

Table 4. Patient data.

Parameter	Patient	
Sex	-	Female
Age	-	75 years
Diagnosis	-	High myopia
	-	Pseudophakia (Intraocular lens, IOL)
	-	Ocular infarction with hemorrhage
	-	Retinal thinning
	-	Retinal detachment in the right eye (OD)
	-	Central scotoma in the right eye (OD)
VA with Rx	-	Left eye (OS): 10/100
	-	With 440 filter: 10/80
CS with Rx	-	6 cpd (cycles per degree) level 8

After applying the best correction with spectacles in both eyes, visual acuity was evaluated with ophthalmic lenses using the LEA numbers, which is specifically designed for patients diagnosed with low vision (Figure 9). According to the International Classification of Diseases (ICD-11), the patient was classified with moderate low vision. These results indicated that the patient could see at 10 feet (3 m) what a person with normal vision could see at 100 feet (30 m) (Table 4). The LV patient reported an improvement of one line of visual acuity when using the ophthalmic filter.

Optical aids must be adapted after applying the best correction to the eye with the best visual acuity. In this case, the 3D-printed Galilean telescope was adapted to the left eye. Before visual acuity measurements were taken, the patient was provided with detailed instructions for manipulating the telescopes. Additionally, the device could be

used until the patient felt comfortable and was able to correctly focus on the optotypes in the LEA numbers. For the two N-BK7 glass lenses, the patient gained a visual acuity of 10/40, while for the 3D-printed GT, the patient's visual acuity improved to 10/32. The two instruments enhanced the patient's visual acuity: the glass lens telescope showed an improvement of 4 lines, while the resin lens telescope achieved 5 lines of improvement in visual acuity. Before adapting the telescopes, the patient's contrast sensitivity was measured using the FACT (Functional Acuity Contrast Test). A 6 cpd level 8 value for the left eye (LE) was obtained, indicating inadequate functional vision, which limited her daily activities (Table 5). Contrast sensitivity is crucial for daily life, as it relates to facial recognition, navigating stairs, and, in general, the recognition of distances and objects. The contrast sensitivity in the left eye significantly improved after adapting the Galilean telescopes for the patient. The resin lens and the N-BK7 glass lens achieved a value of 18 cpd level 4 (Table 5).

Figure 9. Clinical functionality tests.

Table 5. Clinical functionality values.

Test	Non Telescope	Glass Telescope	Resin Telescope
Visual acuity (VA)	10/100	10/40	10/32
Contrast sensitivity (CS)	6 cpd level 8	18 cpd level 4	18 cpd level 4

As can be seen, the patient showed significant improvements after the telescopes were adapted, achieving visual acuity and sensitivity contrast values within the normal range, demonstrating the clinical functionality of the instruments.

5. Discussion

The development of a 3D-printed Galilean telescope for low-vision patients represents a significant innovation in the field of accessible optical aids. This work serves as proof of concept, demonstrating the fabrication method, clinical functionality, and ergonomic feasibility of designing low-cost solutions for visual rehabilitation using additive manufacturing technologies. Unlike existing commercial devices, which often require specialized manufacturing processes and involve high costs [40–43], this proposal focuses on equitable access to technology, making it accessible to both vulnerable and nonvulnerable populations. A cost comparison between commercial BK7 glass lenses and 3D-printed lenses shows that the commercial lenses (objective and eyepiece) cost approximately $50.00 (USD), while the 3D-printed lenses (objective and eyepiece) cost $27.00 (USD), representing a cost savings of approximately 46%. It is important to note that the commercial lenses' cost reflects large-scale manufacturing by a supplier, whereas our 3D-printed lenses' cost corresponds to the production of two pieces. Therefore, if produced at scale, the cost of 3D-printed

lenses could be reduced even further, reinforcing their potential for low-cost, accessible optical solutions.

From the optical functionality analysis, the 3D-printed GT achieved a resolution of 4.0 lp/mm, which enables the identification of fine details, an essential feature for visually impaired individuals [44]. This performance level reinforces the validity of the proposed approach.

Clinically, substantial improvements were observed in visual acuity (from 10/80 to 10/32) and contrast sensitivity (from 6 cpd level 8 to 18 cpd level 4), translating into real functional gains for the patient. These results are consistent with previous studies demonstrating the efficacy of telescopes as optical aids in low-vision populations [33], with the difference that this is an affordable and customizable 3D-printed system.

Beyond optical and clinical performance, this proof of concept also integrates ergonomic considerations into the design. Patients reported that the shape of the telescope's tube facilitated grip, reduced the risk of slipping, and allowed for intuitive use. This user-centered design approach, particularly important for individuals with sensory impairments, marks a significant improvement. Moreover, a comparison of the lens weights demonstrated that the two BK7 glass lenses weighed 28.684 g, whereas the two resin lenses weighed 21.9 g, resulting in a 26.82% reduction in lens relative weight. This reduction contributes to a lighter overall device, further enhancing comfort and usability for the patient.

This initiative also directly contributes to the achievement of the Sustainable Development Goal 3 (Good Health and Well-being) by providing a functional and affordable visual rehabilitation tool with the potential for local production and distribution, even in resource-limited settings. These kinds of solutions are key to advancing universal health coverage, as they combine technological innovation with health equity. We seek to further develop this proposal so that, in the future, these prototypes can be donated to low-income individuals to help improve their quality of life, either temporarily while they secure the resources to obtain specialized equipment or even permanently as a viable long-term alternative.

Despite all of its advantages, this proof of concept has certain limitations. The small clinical sample size prevents immediate generalization of the results. Broader comparative validation with mid- and high-end commercial devices is needed, along with long-term durability and performance testing. Further research into advanced optical materials and optimization of multi-component 3D-printed designs could provide valuable future directions. These developments may lead to improved durability and greater resistance to scratches and surface defects in resin-based optics, making them more comparable to traditional glass components. Also, recent advances in 2-photon polymerization (2PP) have demonstrated outstanding surface quality and submicron resolution in 3D-printed optical components. Although currently limited by cost and fabrication volume, the integration of 2PP could significantly improve the surface accuracy and optical performance of future designs [45–47].

On the other hand, we are currently working on developing a novel surface finishing technique to eliminate the need for conventional polishing. This future advancement aims to further reduce manufacturing costs and simplify the overall production process, ultimately enabling more efficient and accessible production of high-quality optical components.

6. Conclusions

A 3D-printed Galilean telescope for low-vision patients is presented that is lightweight and economical, with easy, precise, and rapid manufacturing, and fabricated using additive technology. The optical performance of the 3D-printed GT showed the power to discern fine

details, with a value of 4.0 lp/mm in optical resolution. Clinical functionality tests showed that when the 3D-printed GT was adapted to the LV patient, visual acuity increased by up to 4 lines on the LEA numbers, from 10/80 to 10/32. The 3D-printed GT telescope also enhanced the patient's contrast sensitivity, improving it from 6 cpd level 8 to 18 cpd level 4. The patient showed significant improvements after the telescope was adapted, achieving visual acuity and sensitivity contrast values within the normal range, demonstrating the clinical functionality of the instrument as a proof of concept.

Supplementary Materials: The following supporting information can be downloaded at: https://www.mdpi.com/article/10.3390/photonics12080815/s1.

Author Contributions: Conceptualization, D.A.-A. and M.I.R.-R.; methodology, D.A.-A., M.I.R.-R., I.M.-J., R.E.H.-C. and R.I.-P.; formal analysis, D.A.-A., M.I.R.-R. and R.D.-U.; experiments, D.A.-A., M.I.R.-R., I.M.-J., R.E.H.-C. and B.V.-M.; writing—original draft preparation, B.V.-M.; writing—review and editing, ALL; supervision, D.A.-A. and M.I.R.-R.; project administration, D.A.-A. and R.D.-U.; funding acquisition, D.A.-A. and R.D.-U. All authors have read and agreed to the published version of the manuscript.

Funding: This research was funded by DGAPA-UNAM (PAPIIT, grant numbers IT104225 and IT104725) and by SECIHTI (LaNOV, grant number LNC-2023-121).

Data Availability Statement: No new data were created or analyzed in this study. Data sharing is not applicable to this article.

Acknowledgments: Itzel Muñoz Juárez acknowledges the grant from ICAT-DGAPA-UNAM.

Conflicts of Interest: The authors declare no conflicts of interest.

References

1. WHO. World Report on Vision. 2020. Available online: https://iris.who.int/bitstream/handle/10665/328717/9789241516570-eng.pdf?sequence=18 (accessed on 20 February 2023).
2. WHO. Eye Care in Health Systems Guide for Action. 2022. Available online: https://iris.who.int/bitstream/handle/10665/354382/9789240050068-eng.pdf?sequence=1 (accessed on 10 May 2024).
3. Wong, W.L.; Su, X.; Li, X.; Cheung, C.M.; Klein, R.; Cheng, C.Y.; Wong, T.Y. Global prevalence of age-related macular degeneration and disease burden projection for 2020 and 2040: A systematic review and meta-analysis. *Lancet Glob. Health* **2014**, *2*, e106–e116. [CrossRef] [PubMed]
4. WHO. International Classification of Diseases, 11th Revision. 2018. Available online: https://icd.who.int/en/ (accessed on 1 February 2025).
5. Flaxman, S.R.; Bourne, R.R.A.; Resnikoff, S.; Ackland, P.; Braithwaite, T.; Cicinelli, M.V.; Das, A.; Jonas, J.B.; Keeffe, J.; Kempen, J.H.; et al. Global causes of blindness and distance vision impairment 1990–2020: A systematic review and meta-analysis. *Lancet Glob. Health* **2017**, *5*, e1221–e1234. [CrossRef] [PubMed]
6. Bourne, R.R.A.; Stevens, G.A.; White, R.A.; Smith, J.L.; Flaxman, S.R.; Price, H.; Jonas, J.B.; Keeffe, J.; Leasher, J.; Naidoo, K.; et al. Causes of vision loss worldwide, 1990–2010: A systematic analysis. *Lancet Glob. Health* **2013**, *1*, E339–E349. [CrossRef]
7. Tham, Y.C.; Li, X.; Wong, T.Y.; Quigley, H.A.; Aung, T.; Cheng, C.Y. Global prevalence of glaucoma and projections of glaucoma burden through 2040: A systematic review and meta-analysis. *Ophthalmology* **2014**, *121*, 2081–2090. [CrossRef]
8. Fricke, T.R.; Tahhan, N.; Resnikoff, S.; Papas, E.; Burnett, A.; Ho, S.M.; Naduvilath, T.; Naidoo, K.S. Global Prevalence of Presbyopia and Vision Impairment from Uncorrected Presbyopia: Systematic Review, Meta-analysis, and Modelling. *Ophthalmology* **2018**, *125*, 1492–1499. [CrossRef]
9. National Research Council (US) Committee on Disability Determination for Individuals with Visual Impairments. *Visual Impairments: Determining Eligibility for Social Security Benefits*; Lennie, P., Van Hemel, S.B., Eds.; National Academies Press: Washington, DC, USA, 2002.
10. Kv, V.; Vijayalakshmi, P. Understanding definitions of visual impairment and functional vision. *Community Eye Health* **2020**, *33*, S16–S17.
11. European Council of Optometry and Optics. Low Vision. 2011. Available online: https://www.ecoo.info/wp-content/uploads/2012/09/ECOO-Position-Paper-Low-Vision-FINAL.pdf (accessed on 20 February 2025).

12. Scott, I.U.; Smiddy, W.E.; Schiffman, J.; Feuer, W.J.; Pappas, C.J. Quality of life of low-vision patients and the impact of low-vision services. *Am. J. Ophthalmol.* **1999**, *128*, 54–62. [CrossRef]

13. Corn, A.L.; Erin, J.N. *Foundations of Low Vision: Clinical and Functional Perspectives*, 2nd ed.; AFB Press: New York, NY, USA, 2010.

14. Jose, R.T. (Ed.) *Understanding Low Vision*; AFB Press: New York, NY, USA, 2004.

15. Wu, Y.; Liu, J.; Kang, L.; Tian, J.; Zhang, X.; Hu, J.; Huang, Y.; Liu, F.; Wang, H.; Wu, Z. An overview of 3D printed metal implants in orthopedic applications: Present and future perspectives. *Heliyon* **2023**, *9*, e17718. [CrossRef] [PubMed]

16. Rankin, T.M.; Giovinco, N.A.; Cucher, D.J.; Watts, G.; Hurwitz, B.; Armstrong, D.G. Three-dimensional printing surgical instruments: Are we there yet? *J. Surg. Res.* **2014**, *189*, 193–197. [CrossRef]

17. He, Y.; Xue, G.; Fu, J. Fabrication of low cost soft tissue prostheses with the desktop 3D printer. *Sci. Rep.* **2014**, *4*, 6973. [CrossRef]

18. Bhatti, S.S.; Singh, J. 3D printing of biomaterials for biomedical applications: A review. *Int. J. Interact. Des. Manuf.* **2023**. [CrossRef]

19. Atala, A. Introduction: 3D Printing for Biomaterials. *Chem. Rev.* **2020**, *120*, 10545–10546. [CrossRef] [PubMed]

20. Grygier, D.; Kujawa, M.; Kowalewski, P. Deposition of Biocompatible Polymers by 3D Printing (FDM) on Titanium Alloy. *Polymers* **2022**, *14*, 235. [CrossRef] [PubMed]

21. Aguirre-Aguirre, D.; Gonzalez-Utrera, D.; Villalobos-Mendoza, B.; Díaz-Uribe, R. Fabrication of biconvex spherical and aspherical lenses using 3D printing. *Appl. Opt.* **2023**, *62*, C14–C20. [CrossRef] [PubMed]

22. Alam, F.; Ali, M.; Elsherif, M.; Salih, A.E.; El-Atab, N.; Butt, H. 3D printed intraocular lens for managing the color blindness. *Addit. Manuf. Lett.* **2023**, *5*, 100129. [CrossRef]

23. Zhu, Y.; Tang, T.; Zhao, S.; Joralmon, D.; Poit, Z.; Ahire, B.; Keshav, S.; Rajendra Raje, A.; Blair, J.; Zhang, Z.; et al. Recent advancements and applications in 3D printing of functional optics. *Addit. Manuf.* **2022**, *52*, 102682. [CrossRef]

24. Bautista-Hernández, A.; Villalobos-Mendoza, B.; Pérez-Tijerina, E.; Aguirre-Aguirre, D. Study and characterization of components fabricated in a 3D printer. *J. Phys. Conf. Ser.* **2022**, *2307*, 012026. [CrossRef]

25. Gonzalez-Utrera, D.; Villalobos-Mendoza, B.; Aguirre-Aguirre, D. Fabrication of Alvarez Lenses Prototypes Using a 3D Printer. In *Frontiers in Optics + Laser Science 2022 (FIO, LS), Technical Digest Series*; Optica Publishing Group: Washington, DC, USA, 2022; p. JW5B.9. [CrossRef]

26. Aguirre-Aguirre, D.; Gonzalez-Utrera, D.; Villalobos-Mendoza, B.; Campos-Garcia, M. Biconvex Lens Fabrication Using a 3D Printer. In *Frontiers in Optics + Laser Science 2022 (FIO, LS), Technical Digest Series*; Optica Publishing Group: Washington, DC, USA, 2022; p. JW4B.2. [CrossRef]

27. Gonzalez-Utrera, D.; Villalobos-Mendoza, B.; Diaz-Uribe, R.; Aguirre-Aguirre, D. Modeling, fabrication, and metrology of 3D printed Alvarez lenses prototypes. *Opt. Express* **2024**, *32*, 3512–3527. [CrossRef]

28. Bautista-Hernández, A.M.; Villalobos-Mendoza, B.; Izazaga-Pérez, R.; Solís-Pomar, F.; Gutiérrez-Lazos, C.D.; Aviles-Alvarado, A.; Garcia-Castillo, F.A.; Pérez-Tijerina, E.G.; Aguirre-Aguirre, D. Design and fabrication of a lightweight 3D first surface mirror aluminized by DC magnetron sputtering. *Appl. Opt.* **2023**, *62*, 9089–9095. [CrossRef]

29. Formlabs. Form3+ Rapid, Flawless Prints Every Time. Available online: https://formlabs.com/3d-printers/form-3/ (accessed on 10 May 2024).

30. Mendes-Felipe, C.; Patrocinio, D.; Laza, J.M.; Ruiz-Rubio, L.; Vilas-Vilela, J.L. Evaluation of postcuring process on the thermal and mechanical properties of the Clear02™ resin used in stereolithography. *Polym. Test.* **2018**, *72*, 115–121. [CrossRef]

31. Berglund, D.G.; Tkaczyk, S.T. Fabrication of optical components using a consumer-grade lithographic printer. *Opt. Express* **2019**, *27*, 30405–30420. [CrossRef] [PubMed]

32. Peli, E.; Vargas-Martin, F. In-the-spectacle-lens telescopic device. *J. Biomed. Opt.* **2008**, *13*, 034027. [CrossRef]

33. Choyce, P. A Galilean telescope using an anterior-chamber implant as eyepiece. *Lancet* **1963**, *281*, 794–796. [CrossRef]

34. Vincent, S.J. The use of contact lens telescopic systems in low vision rehabilitation. *Contact Lens Anterior Eye* **2017**, *40*, 131–142. [CrossRef] [PubMed]

35. Safrani, A.; Abdulhalim, I. Real-time phase shift interference microscopy. *Opt. Lett.* **2014**, *39*, 5220–5223. [CrossRef]

36. Tien, C.L.; Lin, H.Y.; Chang, C.K.; Tang, C.J. Effect of Oxygen Flow Rate on the Optical, Electrical, and Mechanical Properties of DC Sputtering ITO Thin Films. *Adv. Condens. Matter Phys.* **2018**, 2647282. [CrossRef]

37. Assefa, B.G.; Saastamoinen, T.; Pekkarinen, M.; Biskop, J.; Nissinen, V.; Kuittinen, M.; Turunen, J.; Saarinen, J. Realizing freeform optics using 3d-printer for industrial based tailored irradiance distribution. *OSA Contin.* **2019**, *2*, 690–702. [CrossRef]

38. Muñoz-Juárez, I.; Rodríguez-Rodríguez, M.I.; Zarco-López, D.T.; Hernández-Carbajal, R.E.; Izazaga-Pérez, R.; Aguirre-Aguirre, D. Desempeño de telescopios galileanos híbridos en pacientes con diagnóstico de baja visión. *ACONTACS* **2024**, *6*, 136–144.

39. Muñoz-Juárez, I.; Rodríguez-Rodríguez, M.I.; Aguirre-Aguirre, D.; Hernández-Carbajal, R.E. Desempeño de telescopios galileanos en pacientes informados con diagnóstico de baja visión. *ACONTACS* **2023**, *5*, 62–72.

40. İdil, A.; Şahli, E. *Pediatric Vitreoretinal Surgery. Low Vision Aids*; Springer: Cham, Switzerland, 2023; pp. 1059–1078.

41. Fok, D.; Polgar, J.M.; Shaw, L.; Jutai, J.W. Low vision assistive technology device usage and importance in daily occupations. *Work* **2011**, *39*, 37–48. [CrossRef]

42.   Naidoo, K.S.; Maharaj, Y.I.; Pillay, V.; Fellhauer, S. Optical products for refractive error and low vision. *Community Eye Health* **2011**, *24*, 42–43. [PubMed]

43.   Karnani, A.G.; Garrette, B.; Kassalow, J.S.; Lee, M. Better Vision for the Poor. *Stanf. Soc. Innov. Rev.* **2011**, *9*, 66–71. [CrossRef]

44.   Sumalini, R.; Satgunam, P. *Ophthalmic Diagnostics. Visual Acuity: High Contrast and Low Contrast*; Springer: Singapore, 2024; pp. 1–14.

45.   Ovsianikov, A.; Farsari, M.; Chichkov, B.N. *Photonic and Biomedical Applications of the Two-Photon Polymerization Technique. Stereolithography*; Springer: Boston, MA, USA, 2011; pp. 257–297.

46.   Singhal, A.; Dalmiya, A.; Lynch, P.T.; Paprotny, I. 2-Photon Polymerized IP-Dip 3D Photonic Crystals for Mid IR Spectroscopic Applications. *IEEE Photonics Technol. Lett.* **2023**, *35*, 410–413. [CrossRef]

47.   Thompson, J.R.; Worthington, K.S.; Green, B.J.; Mullin, N.K.; Jiao, C.; Kaalberg, E.E.; Wiley, L.A.; Han, I.C.; Russell, S.R.; Sohn, E.H.; et al. Two-photon polymerized poly(caprolactone) retinal cell delivery scaffolds and their systemic and retinal biocompatibility. *Acta Biomater.* **2019**, *94*, 204–218. [CrossRef]